Journal of Hydraulic Structures
J. Hydraul. Struct., 2024; 10(1): 13-28
DOI: 10.22055/jhs.2024.45772.1281

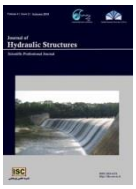

OPEN ACCESS

Experimental evaluation of dune formation downstream of pier scour hole with upstream debris accumulation

Ali Mahdian Khalili [1]
Pouria Akbari Dadamahalleh [1]
Mehdi Hamidi[2]

Abstract

Debris upstream of the bridge pier and through the flow variations, changes scour hole and river morphology. Dune forms downstream of the pier as a result of sediment movement in the pier scour phenomenon. The present study investigates the dune characteristics and geometrical parameters in experimental models. Experimental models are categorized into four cases including the pier, pier with buried debris, pier with free debris, and pier with free debris which was protected by bed sill at four various distances from the pier downstream face. It was concluded that debris submergence, densimetric particle Froude number, flow intensity, and bed sill affect dune geometrical parameters such as dune height (h_d), dune crest position (x_d), and dune length (l_d). Results show dune height increases with debris accumulation up to almost 150% and its crest distance from the pier reduces up to approximately 100%. Also, in higher F_d, the dune height and its crest distance reduce with bed sill up to 50%, and in lower F_d, h_d, and x_d increase by up to 80% by using bed sill. Based on these effective parameters, three separate equations were proposed for h_d, x_d, and l_d in pier scour with debris accumulation protected by bed sill.

Keywords: Bed sill, Bridge scour, Debris, Dune, Experimental investigation.

Received: 06 January 2024; Accepted: 13 February 2024

1. Introduction

Debris including broken trees, large pieces of wood, and leaves can be transported in river flow as a result of natural hazards such as landslides and floods. These floated materials can accumulate upstream of the bridge pier and block and change the river flow pattern. This phenomenon increases the shear stress and generates a horseshoe vortex, and a wake vortex upstream and downstream of the pier, respectively. Thus, scour hole depth becomes greater and

[1] Faculty of Civil Engineering, Babol Noshirvani University of Technology, Babol, Mazandaran, Iran.
[2] Faculty of Civil Engineering, Babol Noshirvani University of Technology, Babol, Mazandaran, Iran. Email: hamidi@nit.ac.ir **(Corresponding author)**

river morphology varies [1]. The effects of debris accumulation with different shapes were studied on pier scour depth [1-18].

Melville and Dangol (1992) [2] studied the maximum scour depth of the pier (d_s) with various debris blockage shapes resulting in the pier diameter being considered larger than the actual pier diameter. Their suggested equation for the effective pier diameter was corrected by Lagasse et al. [1, 3]. The accumulation of rectangular woody debris upstream of the cylindrical pier increased d_s by up to 30% compared to the accumulating middle of it [4]. Debris with different lengths, thicknesses, shapes, and positions were investigated and it was observed that d_s become larger by increasing the debris thickness, also rectangular debris creates larger ds than triangular, and cylindrical [6]. When the debris approaches the river bed, d_s reduces and the largest value is for the case that debris is exactly below the water elevation [9]. It was concluded that when debris was exactly on the channel bed, it conserved the river bed locally and decreased d_s [6, 9, 11]. The level of debris investigated on pier scour indicated that free debris (upper than the bed level) in all flow depths increases d_s and buried debris (exactly on the bed level) in shallow flow increases ds up to 10% and reduces d_s in partially deep flow [16]. Distances of the pier from the channel wall were studied with debris accumulation and d_s increases when the pier was near the channel wall [12]. Also, the scour hole length increases in cases with debris [12]. At flow with small depth, the location of debris accumulation influences the scour evolution and bed topography but at deep flow, its impact is few [13].

Oliveto and Hager (2014) investigated the dune characteristics generated immediately downstream of local scour piers experimentally [19]. They described dune evolution and its downstream migration by proposing equations as a function of the effective parameters. Pagliara and Carnacina (2010) studied the scour morphology and dune evolution on pier scour with debris accumulation [20]. They suggested a new equation to predict maximum scour depth and longitudinal and transversal lengths.

Many researchers studied scour hole depth and reduced it with some applicable countermeasures such as bed sill, collar, riprap, slot, and submerged vanes [20-35]. Utilizing a buried sill in the channel bed slows the scour rate and reduces d_s in debris accumulation conditions [5]. Slots on the pier reduced scour depth with debris accumulation, and the reduction efficiency in debris cases compared to cases without it did not have constant variations and changes due to different debris shapes [14]. Collar installation on the bridge pier with debris reduced d_s by about 40 percent compared to the case pier only, and also reduction efficiency became 25 percent more in debris accumulation conditions [15]. When riprap is used as a countermeasure, debris does not influence the performance of standard-size riprap [17]. But riprap stone median size is an effective parameter, and with debris accumulation when it was reduced by 25% riprap efficiency was decreased by 10% [17].

Former studies investigated the maximum depth of the pier scour hole in debris cases and suggested different analytical equations to predict it. Dune bed formation is inevitable in the pier scour phenomenon, generated through the deposition of sediment particles from around the pier upstream region of the pier and extending downstream during scour hole evolution and equilibrium times. Although dune evolution is dependent on the geometry of scour holes, a comprehensive study did not apply to investigate dune characteristics, especially in the case of debris blockage. On the other hand, debris increases the scour depth locally, so it is necessary to reduce it by applying some techniques. Since previous studies did not interpret dune formation downstream of the scour hole in local pier scour hole in the case of debris blockage sufficiently and comprehensively, the present study focused on dune formation downstream of the pier scour hole with debris blockage in shapes rectangular in two separate conditions with the sill protected

and without it. As it was reported that debris level is an effective parameter, debris was considered in two different levels including buried (exactly on the bed level) and free (upper than the bed level). Sills were installed at distances of 0D, 1D, 2D, 3D, and 4D downstream of the bridge pier. Finally, three separate equations were suggested based on obtained results for dune height, dune crest position, and dune length.

2. Materials and methods

2.1. Dimensional analysis

Dune height depends on various parameters including sediment parameters and hydraulic parameters. Oliveto and Hager (2014) proposed equation (1) for dune height (h_d) and its distance from pier (x_d) as follows [19]:

$$\frac{h_d}{y}.\frac{x_d}{y} = f(\frac{D}{y}.F_d.\sigma_g.\Delta F_d.\frac{y}{d_{50}}.T) \quad (1)$$

where D is the pier diameter in meter, y is approach flow depth in meters, F_d is densimetric particle Froude number, σ_g is sediment nonuniformity parameter=$(d_{84}/d_{16})^{0.5}$, $\Delta F_d = F_{di}-F_d$ (F_{di} is the inception densimetric Froude number, d_{50} is the median particle size in meter, and T is the dimensionless time= $([(\rho_s-\rho)/\rho]gd_{50})^{0.5}(t/y)$, ρ_s is sediment specific weight in kilogram per cube meter, ρ is water specific weight in kilogram per cube meter, g is gravitational acceleration in meter per square second, and t is time. In the case of debris accumulation with bed sill equation (2) suggested [16]:

$$\frac{h_d}{D}.\frac{x_d}{D}.\frac{l_d}{D} = f\left(\frac{H}{D}.F_d.\frac{u}{u_c}.\frac{L_b}{D}\right) \quad (2)$$

where H is the vertical gap between the debris top surface and sand's initial level in meter, u is the flow velocity depth at the pier upstream in meter per second, u_c is the critical velocity of bed particle in meter per second, and L_b is the bed sill downstream distance from the pier in meter.

2.2. Experimental model

An experimental model was made in a hydraulic laboratory of Noshirvani University of Technology, in Babol, and tests were performed at a sediment flume with length, width, and height of 4, 0.6, and 0.2 meters (Figure 1(a)). For adjusting the flow and tailwater depths, the flume has a tailgate that provides a defined water depth in the channel (Figure 1(b)). To avoid flow disturbance wire mesh plate was located after the upstream tank in the channel inlet and for having developed flow, a 0.5-meter-long rigid apron was installed at the channel beginning (Figure 1(c)) and a cylindrical pier was located 3 meters downstream of the inlet flow which provides a suitable symmetric flow pattern in the channel. A point gauge with an accuracy of 0.1 mm was utilized to measure water and sediment depths (Figure 1(d)).

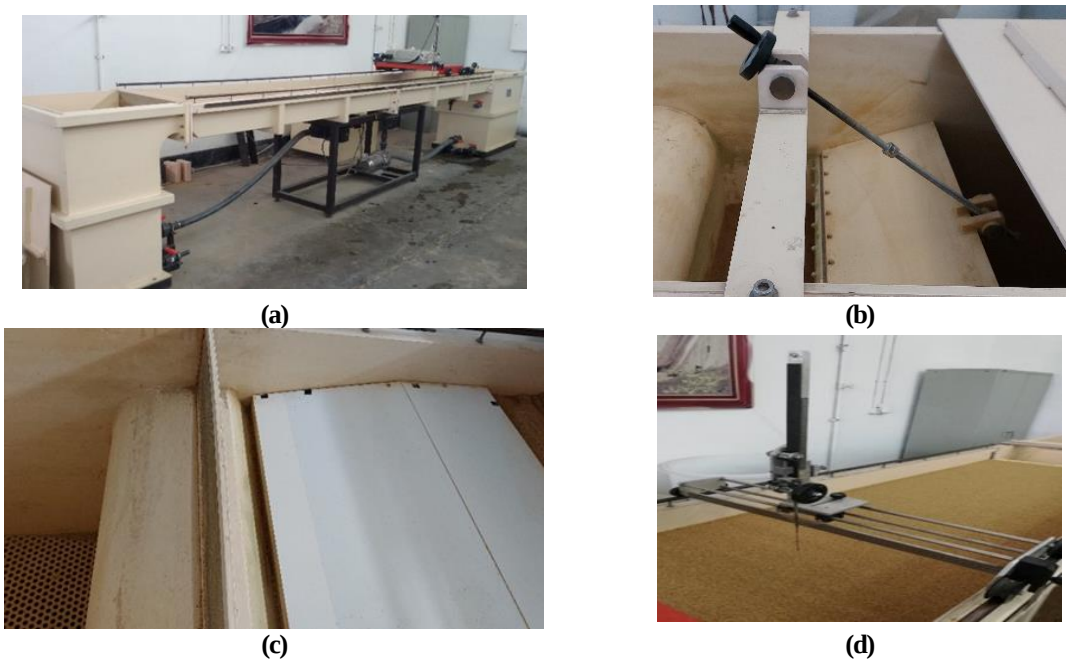

Figure 1. (a) Laboratory flume (b) Tailgate (c) Wire mesh plate and rigid apron (d) Point gauge

To avoid the formation of a ripple, the median particle size (d_{50}) should be smaller than 0.7 mm [36]. When the ratio between channel width to bridge pier diameter (B/D) is more than 6.25, channel walls do not affect scour hole geometry and morphology [36]. If D/d_{50}>20-25, sand size does not influence scour depth [36]. The physical model included bed sediment, a pier, a debris box, and a sill. Tests were applied on sand sediment with parameters according to Figure 2. For sample sediment d_{50}=0.82 mm and σ_g=1.26 (uniform sediment). The pier was made with a steel pipe with a 3 cm diameter welded on an iron plate (B/D=20, D/d_{50}=36.6). When Wooden debris is gathered upstream of the bridge pier, a more possible shape form is a rectangle, and rectangular wooden debris creates maximum scour depth around a pier [9-10]. Debris was modeled as a rectangular mesh wire box 0.05 m high, 0.10 m long, and 0.12 m wide poured with wood pieces with diameters of 0.1 to 0.5 cm and fixed on the pier by a screw. Sill was modeled with a PVC plate that was 0.10 m high, 3 mm thick, and 0.60 m wide located at five varied positions with distances 0D, 1D, 2D, 3D, and 4D, downstream of the pier.

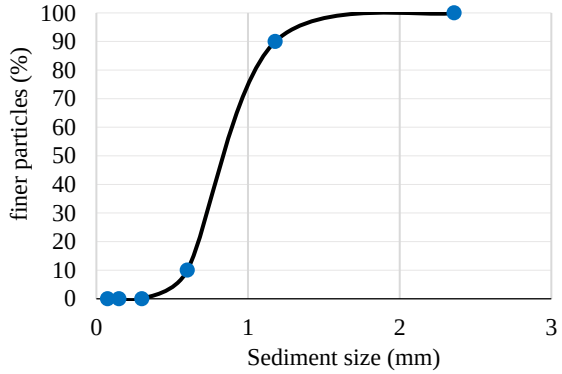

Figure 2. Sand sediment granulation

Table 1 indicates the experimental setup and hydraulic parameters of the model considered in four cases (A, B, C, and D). Case A included a pier, Case B is a pier with buried debris (exactly on the bed level), Case C included a pier with free debris (with a distance of D upper than the bed level), and Case D which bed sill is added to case C with downstream distance of 0D, 1D, 2D, 3D, and 4D. In Table 1, y is the approach flow depth in meters, H is the vertical gap between the debris top surface and the sand's initial level in meters, u is the flow velocity depth at the pier upstream in meters per second, u_c is the critical velocity of bed particle in meter per second, F_d is particle densimetric Froude number, D is the pier diameter in meter, and L_b is the bed sill downstream distance from the pier in meter.

Table 1. Experimental Setup

Case	Model	Test	y (m)	H (m)	y/H	u/uc	F_d	y/D	L_b/D
A	Pier	A1	0.03	NA*	NA	0.838	3.688	1.000	NA
		A2	0.04	NA	NA	0.599	2.398	1.333	NA
		A3	0.05	NA	NA	0.462	1.719	1.667	NA
		A4	0.06	NA	NA	0.370	1.289	2.000	NA
		A5	0.07	NA	NA	0.311	1.032	2.333	NA
		A6	0.08	NA	NA	0.265	0.842	2.667	NA
		A7	0.09	NA	NA	0.230	0.705	3.000	NA
B	Pier + Buried Debris	B1	0.03	0.05	0.600	0.838	3.688	1.000	NA
		B2	0.04	0.05	0.800	0.599	2.398	1.333	NA
		B3	0.05	0.05	1.000	0.462	1.719	1.667	NA
		B4	0.06	0.05	1.200	0.370	1.289	2.000	NA
		B5	0.07	0.05	1.400	0.311	1.032	2.333	NA
		B6	0.08	0.05	1.600	0.265	0.842	2.667	NA
		B7	0.09	0.05	1.800	0.230	0.705	3.000	NA
C	Pier + Free Debris	C1	0.04	0.08	0.500	0.599	2.398	1.333	NA
		C2	0.05	0.08	0.625	0.462	1.719	1.667	NA
		C3	0.06	0.08	0.750	0.370	1.289	2.000	NA
		C4	0.07	0.08	0.875	0.311	1.032	2.333	NA
		C5	0.08	0.08	1.000	0.265	0.842	2.667	NA
		C6	0.09	0.08	1.125	0.230	0.705	3.000	NA
D	Pier + Free Debris + Sill	D1	0.04	0.08	0.500	0.599	2.398	1.333	0
		D2	0.06	0.08	0.750	0.370	1.289	2.000	0
		D3	0.08	0.08	1.000	0.265	0.842	2.667	0
		D4	0.04	0.08	0.500	0.599	2.398	1.333	1
		D5	0.06	0.08	0.750	0.370	1.289	2.000	1
		D6	0.08	0.08	1.000	0.265	0.842	2.667	1
		D7	0.04	0.08	0.500	0.599	2.398	1.333	2
		D8	0.06	0.08	0.750	0.370	1.289	2.000	2
		D9	0.08	0.08	1.000	0.265	0.842	2.667	2
		D10	0.04	0.08	0.500	0.599	2.398	1.333	3
		D11	0.06	0.08	0.750	0.370	1.289	2.000	3
		D12	0.08	0.08	1.000	0.265	0.842	2.667	3
		D13	0.04	0.08	0.500	0.599	2.398	1.333	4
		D14	0.06	0.08	0.750	0.370	1.289	2.000	4
		D15	0.08	0.08	1.000	0.265	0.842	2.667	4

* Not Available

2.3. Equilibrium scour time

Three tests (A2, B2, and C1) were performed over 8 hours to achieve scour equilibrium time. Figure 3 shows that after 5 hours, scour hole depth remains almost constant for up to 8 hours, thus this time can be considered an equilibrium scour time.

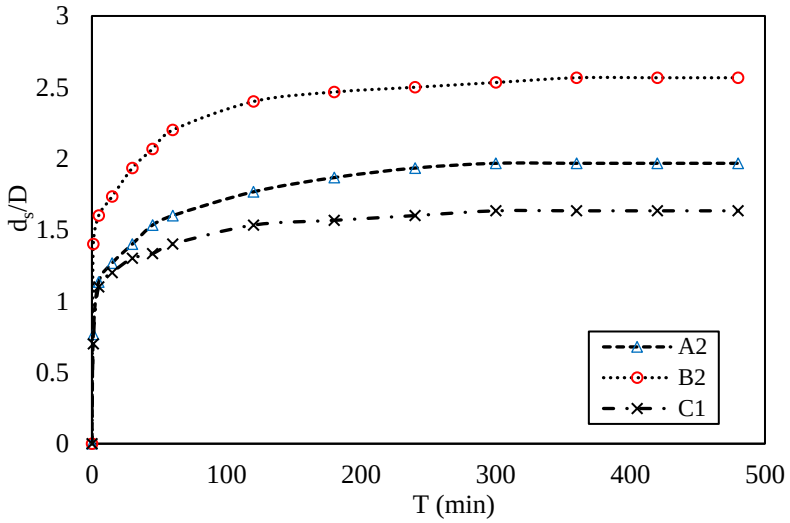

Figure 3. Time evolution of scour hole depth

3. Results and discussion

3.1. Experimental results

In all tests dunes formed downstream of the scour hole of the pier. It occurred through the sand removal around the upstream region of the pier as a result of vortexes and deposition downstream during the scour process. Figure 4 indicates dune formation following a scour hole in the same hydraulic conditions (F_d=2.398) in different cases (test A2, test B2, and Test D10). As can be observed in all conditions including pier (case A), pier with debris (case B and C), and pier with debris protected by sill (case D) dune geometry changes. The dune structure has two wings that develop until reaches the initial bed level, also it has one crest area where dune height is the maximum value.

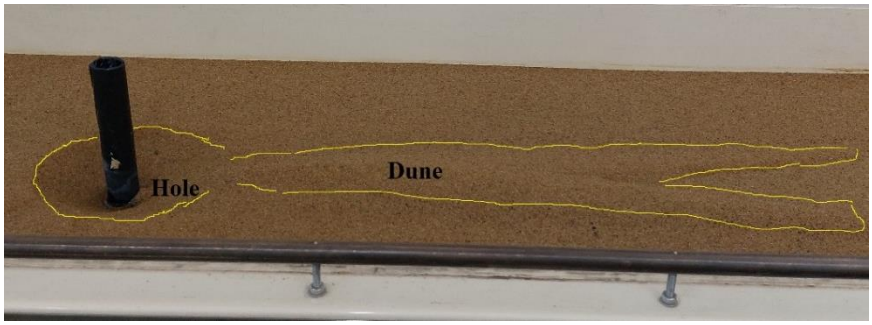

(a)

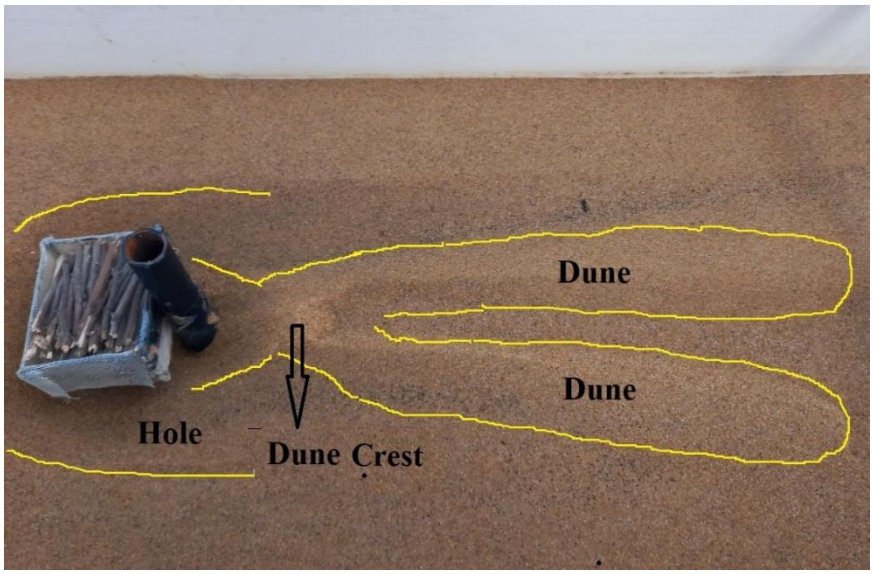

(b)

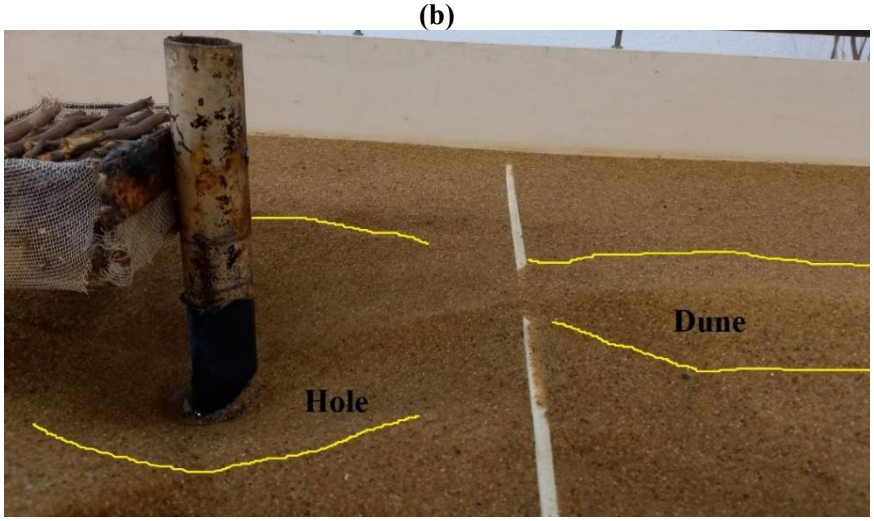

(c)

Figure 4. Dune Formation downstream of scour hole (a) Test A2 (b) Test B2 (c) Test D10

Table 2 presents the results of each test for dune characteristics. h_d is the maximum height of the dune crest in meters (dune height). x_d is the longitudinal distance between the location of the maximum height of the dune crest and the pier downstream face (dune crest position) in meters. l_d is the longitudinal distance between the pier's downstream face and the location where the dune reaches the bed's initial level (dune length) in meters.

Table 2. Dune characteristics

Case	Model	Test	y/H	u/uc	F_d	L_b/D	h_d/D	x_d/D	l_d/D
A	Pier	A1	NA*	0.838	3.688	NA	0.433	15.833	NM**
		A2	NA	0.599	2.398	NA	0.167	5.833	NM
		A3	NA	0.462	1.719	NA	0.300	5.833	NM
		A4	NA	0.370	1.289	NA	0.567	4.167	NM
		A5	NA	0.311	1.032	NA	0.600	3.500	NM
		A6	NA	0.265	0.842	NA	0.333	3.000	NM
		A7	NA	0.230	0.705	NA	0.033	1.167	NM
B	Pier + Buried Debris	B1	0.600	0.838	3.688	NA	0.467	4.167	NM
		B2	0.800	0.599	2.398	NA	0.800	5.833	NM
		B3	1.000	0.462	1.719	NA	0.767	3.500	NM
		B4	1.200	0.370	1.289	NA	0.300	1.500	NM
		B5	1.400	0.311	1.032	NA	0.467	0.500	NM
		B6	1.600	0.265	0.842	NA	0.433	0.500	NM
		B7	1.800	0.230	0.705	NA	0.033	0.033	NM
C	Pier + Free Debris	C1	0.500	0.599	2.398	NA	0.067	5.833	NM
		C2	0.625	0.462	1.719	NA	0.767	9.167	NM
		C3	0.750	0.370	1.289	NA	1.167	4.500	NM
		C4	0.875	0.311	1.032	NA	0.667	2.833	NM
		C5	1.000	0.265	0.842	NA	0.333	1.500	NM
		C6	1.125	0.230	0.705	NA	0.233	2.833	NM
D	Pier + Free Debris + Sill	D1	0.500	0.599	2.398	0	NM	NM	NM
		D2	0.750	0.370	1.289	0	0.367	3.000	4.333
		D3	1.000	0.265	0.842	0	0.333	0.667	5.000
		D4	0.500	0.599	2.398	1	0.700	11.000	25.000
		D5	0.750	0.370	1.289	1	0.967	3.333	4.000
		D6	1.000	0.265	0.842	1	0.600	2.000	5.000
		D7	0.500	0.599	2.398	2	0.767	9.000	20.000
		D8	0.750	0.370	1.289	2	0.800	2.500	3.333
		D9	1.000	0.265	0.842	2	0.400	1.667	5.000
		D10	0.500	0.599	2.398	3	0.967	10.333	26.667
		D11	0.750	0.370	1.289	3	0.833	2.333	4.000
		D12	1.000	0.265	0.842	3	0.433	1.000	5.333
		D13	0.500	0.599	2.398	4	0.800	9.667	30.000
		D14	0.750	0.370	1.289	4	0.600	2.000	4.667
		D15	1.000	0.265	0.842	4	0.400	2.667	5.000

* Not Available

** Not Measured

3.2. Effect of debris on dune characteristics

As can be observed from Table 2, debris submergence, densimetric particle Froude number, flow intensity, and bed sill position can affect dune geometrical parameters. Figures 5 and 6 present debris submergence (y/H) and densimetric particle Froude number on dune height and its position, respectively. It concluded that the variations of dune height and its position did not have a constant relation with debris submergence and densimetric particle Froude number, at first, they increased and then reduced. In cases without debris, x_d/D reduced with increasing F_d, in which means the dune crest is closer to the pier downstream.

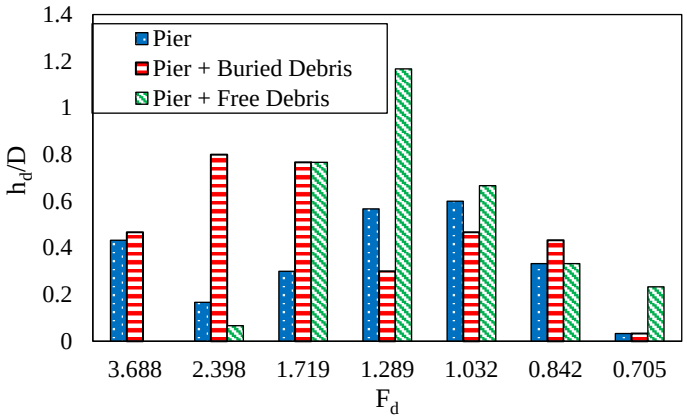

Figure 5. Effect of debris submergence and densimetric particle Froude number on dune height

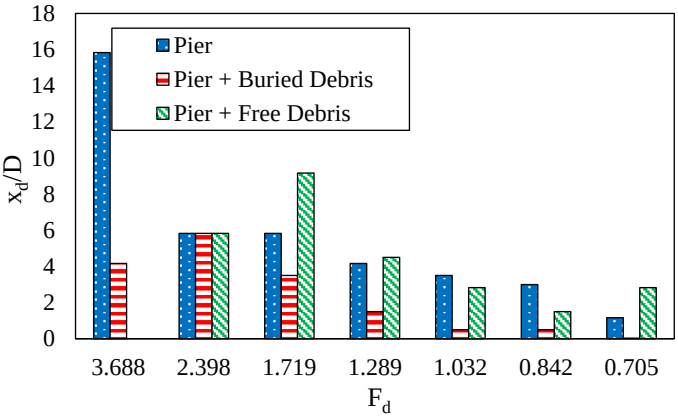

Figure 6. Effect of debris submergence and densimetric particle Froude number on dune position

Figure 7 presents the percentage variations of dune parameters in cases with debris accumulation compared with the cases without it in the same hydraulic parameters. It can be concluded that dune height increases in both buried and free debris and in all hydraulic conditions buried debris reduces x_d which means the dune crest is located closer to the pier.

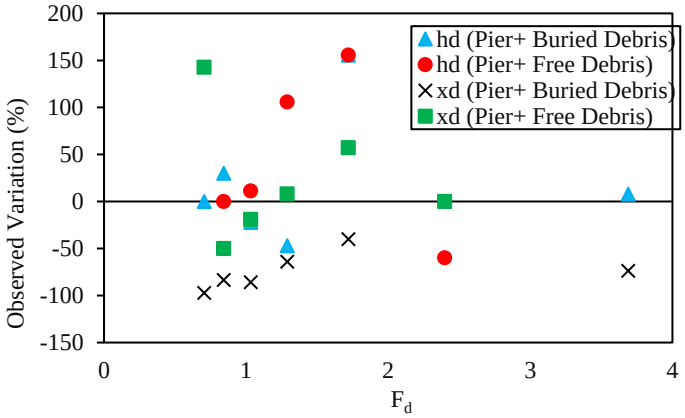

Figure 7. Variations of dune characteristics with debris accumulation compared to cases without it

3.3. Effect of bed sill on dune characteristics

Figures 8, 9, and 10 show the influence of bed sill position with varied densimetric particle Froude numbers on dune height, its position, and dune height respectively. It concluded that the variations of dune height, pick position, and dune length did not have a linear relation with bed sill gap with pier downstream pier and densimetric particle Froude numbers.

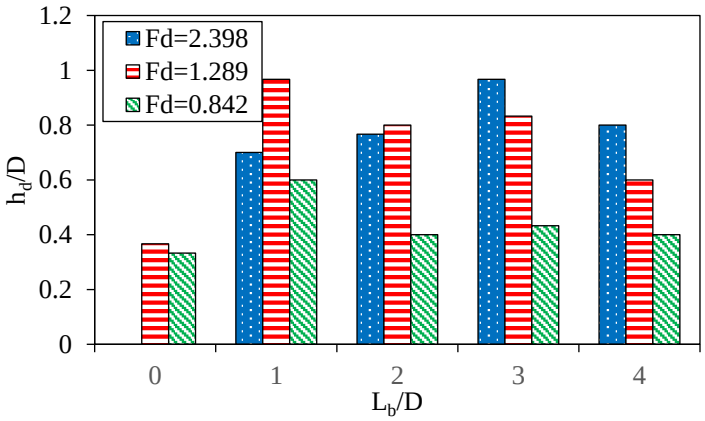

Figure 8. Effect of bed sill position and densimetric particle Froude number on dune height

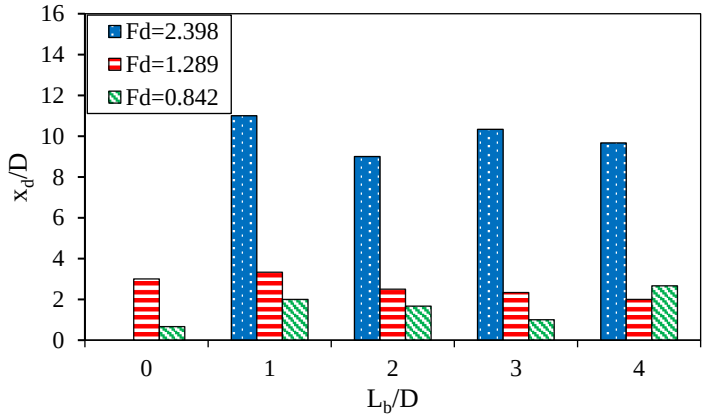

Figure 9. Effect of bed sill position and densimetric particle Froude number on dune position

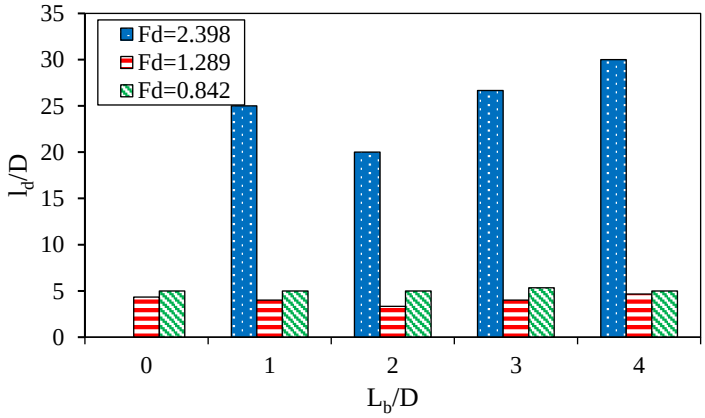

Figure 10. Effect of bed sill position and densimetric particle Froude number on dune length

Figure 11 illustrates the variations of dune parameters when a bed sill is used with free debris in comparison with cases without utilizing bed sill protection. It is observed that hydraulic condition and densimetric particle Froude number affect the influence of bed sill. In higher F_d, the dune height and its crest distance reduce with bed sill but in lower F_d, h_d, and x_d decrease by using bed sill.

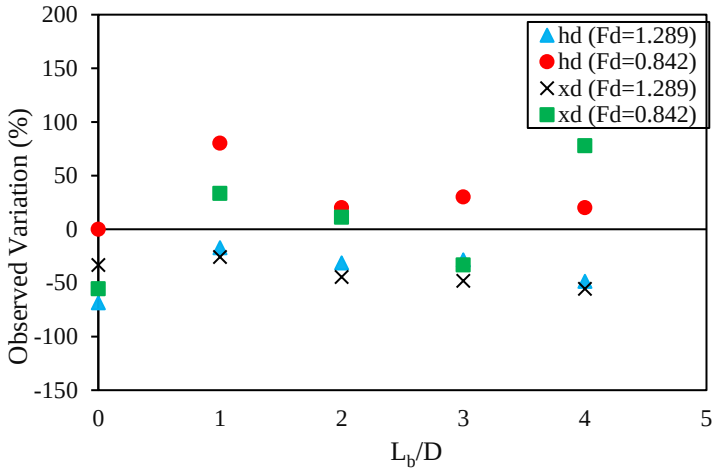

Figure 11. Variations of dune characteristics in debris accumulation with bed sill protection compared to case without sill

3.4. Comparison of obtained dune height with previous results

The obtained results of dimensionless dune height to approach flow depth (h_d/y) were compared to Oliveto and Hager (2014) in Figure 12. This result is for pier scour without debris and bed sill which presents good compatibility with the computed RMSE=0.0421.

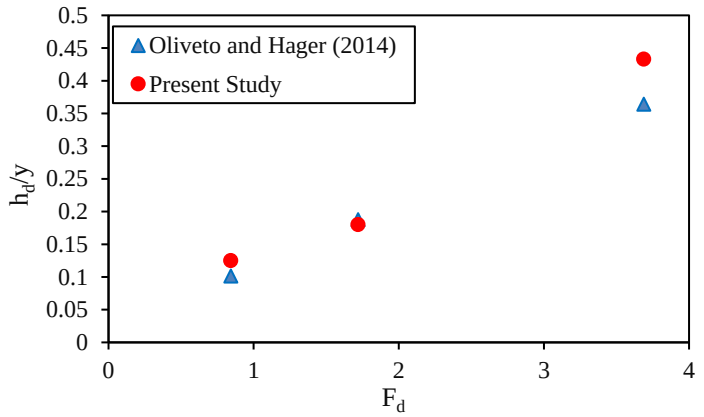

Figure 12. Comparison of obtained dune height in the case without debris and bed sill to the previous study

3.5. Prediction equations for dune characteristics

Based on effective parameters, prediction equations can be proposed by nonlinear regression to analyze extracted data and predict the dune geometry characteristics [37]. Equations (3), (4),

and (5) suggested dune maximum height, dune crest position, and dune maximum length, respectively. These equations were extracted from the Case D model.

$$\frac{h_d}{D} = 1{,}123\left(\frac{y}{H}\right)^{-0{,}132}(F_d)^{0{,}127}\left(\frac{u}{u_c}\right)^{0{,}532}\left(\frac{L_b}{D}\right)^{-0{,}24} \quad (3)$$

$$\frac{x_d}{D} = 14{,}718\left(\frac{y}{H}\right)^{-0{,}147}(F_d)^{0{,}564}\left(\frac{u}{u_c}\right)^{1{,}755}\left(\frac{L_b}{D}\right)^{-0{,}098} \quad (4)$$

$$\frac{l_d}{D} = 2{,}115\left(\frac{y}{H}\right)^{-1{,}307}(F_d)^{1{,}716}\left(\frac{u}{u_c}\right)^{0{,}412}\left(\frac{L_b}{D}\right)^{-0{,}314} \quad (5)$$

Table 3 proposed the parameter ranges and correlation ratio (R^2) for the suggested equations and RMSE as equation (6). In this equation x_p is the predicted values, x_o is the observed values, and n is the data number [38-39].

$$RMSE = \sqrt{\frac{\sum_1^n (x_p - x_o)^2}{n}} \quad (6)$$

Table 3. Effective parameters range for proposed equations

Equation	Parameter	y/H	F_d	u/u_c	L_b/D	RMSE	R^2
1	h_d	0.5-1	0.842-2.398	0.265-0.599	1-4	0.175	0.629
2	x_d	0.5-1	0.842-2.398	0.265-0.599	1-4	0.688	0.984
3	l_d	0.5-1	0.842-2.398	0.265-0.599	1-4	3.052	0.969

Figures 13, 14, and 15 present predictions of dune maximum height, dune crest position, and dune maximum height according to Equations (3), (4), and (5), respectively.

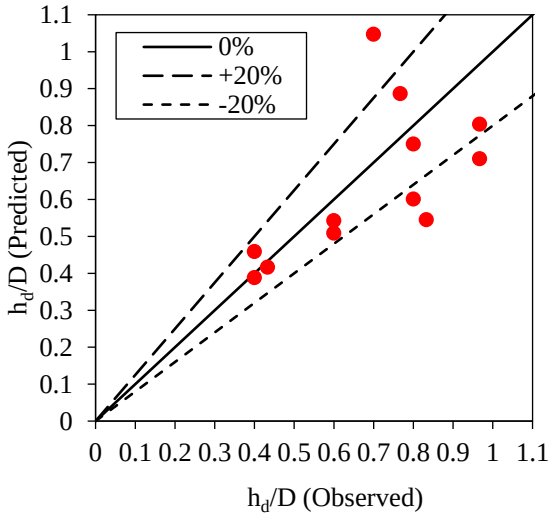

Figure 13. Prediction of dune maximum height

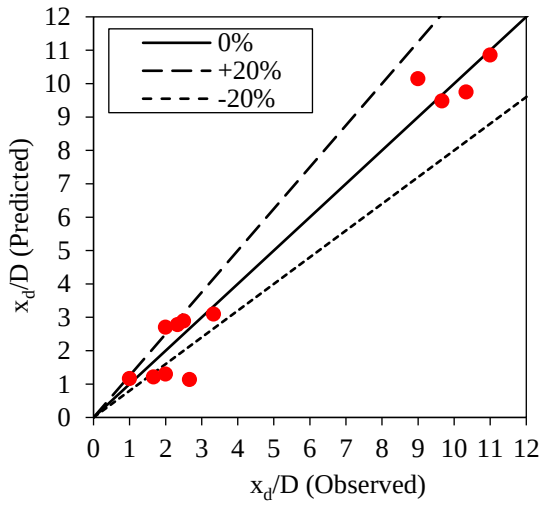

Figure 14. Prediction of dune crest position

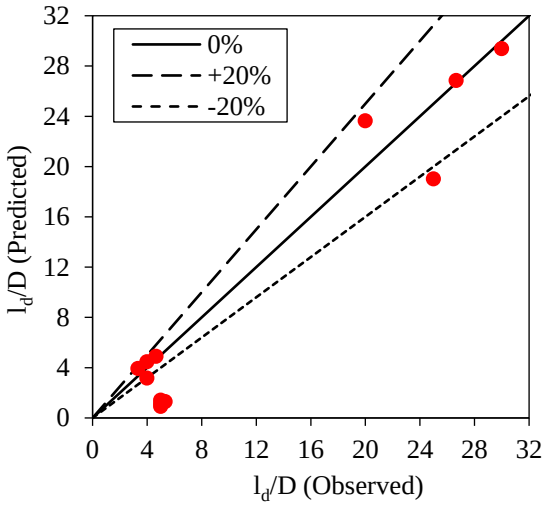

Figure 15. Prediction of dune maximum length

4. Conclusion

The present paper studied the laboratory model for the investigation of scour around the bridge pier with a rectangular upstream block with and without protection of sill. Four cases consist of A (pier), B (pier + buried debris), C (pier + free debris), and D (pier + free debris + bed sill). Dune geometrical parameters such as dune maximum height (h_d), dune crest position (x_d), and dune maximum length (l_d) were measured and compared in each test. It was observed that debris submergence (y/H), densimetric Froude number (F_d), flow intensity (u/u_c), and bed sill position (L_b/D) affect dune geometrical parameters. Results indicated that changes in h_d and x_d did not have a fixed relation with y/H and F_d, at first, they increased and then reduced. When debris did not appear x_d reduced with increasing F_d, it means the dune crest approached the pier downstream. Based on experimental data, equations were achieved on nonlinear regression for debris accumulation with bed sill protected for h_d, x_d, and l_d with a correlation ratio (R^2) equal to

0.629, 0.984, and 0.969, respectively. Used effective parameters in prediction equations have limited ranges which were presented in the results.

References

1. Lagasse PF, Clopper PE, Zevenbergen LW, (2010). Effects of debris on bridge pier scour. NCHRP Report 653, Transportation Research Board, National Academies of Science, Washington, D.C.
2. Melville BW, Dongol DM, (1992). Bridge pier scour with debris accumulation. Journal of Hydraulic Engineering, 118, pp: 1306–1310. https://doi.org/10.1061/(ASCE)0733-9429(1992)118:9(1306).
3. Lagasse PF, Zevenbergen LW, Clopper PE, (2010). Impacts of debris on bridge pier scour. Scour and Erosion. American Society of Civil Engineers, Reston, VA, pp: 854–863.
4. Pagliara S, Carnacina I, (2010). Temporal scour evolution at bridge piers: effect of wood debris roughness and porosity. Journal of Hydraulic Research, 48(1), pp: 3-13. https://doi.org/10.1080/00221680903568592.
5. Pagliara S, Carnacina I, Cigni F, (2010). Sills and gabions as countermeasures at bridge pier in presence of debris accumulations. Journal of Hydraulic Research, 48(6), pp: 764-774. https://doi.org/10.1080/00221686.2010.528184.
6. Pagliara S, Carnacina I, (2011). Influence of wood debris accumulation on bridge pier scour. Journal of Hydraulic Engineering, 137, pp: 254–261. https://doi.org/10.1061/(ASCE)HY.1943-7900.000028.
7. Pagliara S, Carnacina I, (2011). Influence of large woody debris on sediment scour at bridge pier. International Journal of Sediment Research, 26, pp: 121-136. https://doi.org/10.1016/S1001-6279(11)60081-4.
8. Park JH, Sok C, Park CK, Do KY, (2016). A study on the effects of debris accumulation at sacrificial piles on bridge pier scour: I. Experimental Results. KSCE Journal of Civil Engineering, 20, pp: 1546–1551. https://doi.org/10.1007/s12205-015-0207-5.
9. Rahimi E, Qaderi K, Rahimpour M, Ahmadi, MM, (2018). Effect of debris on piers group scour: an experimental study. KSCE Journal of Civil Engineering, 22, pp: 1496–1505. https://doi.org/10.1007/s12205-017-2002-y.
10. Abousaeidi Z, Ghaderi K, Rahimpour M, Ahmadi MM, (2018). Experimental investigation of the effect of debris accumulation on the local scour at bridge pier and abutment. Journal of Water and Soil Conservation, 25(2), pp: 267-282. 10.22069/JWSC.2018.12472.2714.
11. Ebrahimi M, Kripakaran P, Prodanović DM, et al., (2018). Experimental study on scour at a sharp-nose bridge pier with debris blockage. Journal of Hydraulic Engineering, 144:04018071. https://doi.org/10.1061/(ASCE)HY.1943-7900.0001516.
12. Pagliara S, Palermo M, (2020). Effects of bridge pier location and debris accumulation on equilibrium morphology. World Environmental and Water Resources Congress.
13. Palermo M, Pagliara S, Roy D, (2021). Effect of debris accumulation on scour evolution at bridge pier in bank proximity. Journal of Hydrology and Hydromechanics, 61, pp: 1-11. https://doi.org/10.2478/johh-2020-0041.

14. Hamidifar H, Mohammad Ali Nezhadian D, Carnacina I, (2022). Experimental study of debris-induced scour around a slotted bridge pier. Acta Geophysica, 70, pp: 2325–2339. https://doi.org/10.1007/s11600-021-00722-2.
15. Hamidifar H, Shahabi-Haghighi SMB, Chiew YM, (2022). Collar performance in bridge pier scour with debris accumulation. International Journal of Sediment Research, 37, pp: 328-334. https://doi.org/10.1016/j.ijsrc.2021.10.002.
16. Akbari Dadamahalleh P, Hamidi M, Mahdian Khalili A, (2022). Experimental Prediction of the Bed Profile with the Full-submerged and Semi-submerged Debris Accumulation Upstream of the Cylindrical Bridge Pier. Journal of Water and Soil Conservation, 29(4), pp: 95-114. 10.22069/JWSC.2023.20642.3582.
17. Zanganeh-Inaloo F, Hamidifar H, Oliveto G, (2023). Local scour around riprap-protected bridge piers with debris accumulation. Iran. J. Sci. Technol. Trans. Civ. Eng., 47(4), pp: 2393-2408. https://doi.org/10.1007/s40996-023-01034-9.
18. Mahdian Khalili A, Hamidi M, Akbari Dadamahalleh P, (2023). Scour Morphology around the Bridge Pier with Upstream Rectangular Debris. 22nd Iranian Conference on Hydraulics, 8-9 November 2023, University of Maragheh.
19. Oliveto G, Hager WH, (2014). Morphological evolution of dune-like bed forms generated by bridge scour. Journal of Hydraulic Engineering, 140(5), 06014009. https://doi.org/10.1061/(ASCE)HY.1943-7900.0000853.
20. Pagliara S, Carnacina I, (2010). Scour and dune morphology in presence of large wood debris accumulation at bridge pier. In River Flow (Vol. 2, pp. 1223-1230).
21. Chiew YM, (1992). Scour protection at bridge piers. Journal of Hydraulic Engineering, 118, pp: 1260–1269. https://doi.org/10.1061/(ASCE)0733-9429(1992)118:9(1260).
22. Zarrati AR, Chamani MR, Shafaie A, Latifi M, (2010). Scour countermeasures for cylindrical piers using riprap and combination of collar and riprap. International Journal of Sediment Research, 25, pp: 313-322. https://doi.org/10.1016/S1001-6279(10)60048-0.
23. Grimaldi C, Gaudio R, Calomino F, Cardoso AH, (2009). Control of scour at bridge piers by a downstream bed sill. Journal of Hydraulic Engineering, 135, pp: 13–21. https://doi.org/10.1061/(ASCE)0733-9429(2009)135:1(13).
24. Grimaldi C, Gaudio R, Calomino F, Cardoso, AH, (2009). Countermeasures against local scouring at bridge piers: slot and combined system of slot and bed sill. Journal of Hydraulic Engineering, 135, pp: 425–431. https://doi.org/10.1061/(ASCE)HY.1943-7900.0000035.
25. Tafarojnoruz A, Gaudio R, Calomino F, (2012). Bridge pier scour mitigation under steady and unsteady flow conditions. Acta Geophysica, 60, pp: 1076-1097. https://doi.org/10.2478/s11600-012-0040-x.
26. Khaple S, Hanmaiahgari PR, Gaudio R, Dey S, (2017). Splitter plate as a flow-altering pier scour countermeasure. Acta Geophysica, 65, pp: 957–975. https://doi.org/10.1007/s11600-017-0084-z.
27. Pandey M, Azamathulla HM, Chaudhuri S, Pu JH, Pourshahbaz H, (2020). Reduction of time-dependent scour around piers using collars. Ocean Engineering, 213, 107692. https://doi.org/10.1016/j.oceaneng.2020.107692.

28. Raeisi N, Ghomeshi M, (2021). A laboratory study of the effect of asymmetric-lattice collar shape and placement on scour depth and flow pattern around the bridge pier. Water Supply 22, pp: 734-748. https://doi.org/10.2166/ws.2021.239.
29. Saad NY, Fattouh EM, Mokhtar M, (2021). Effect of L-shaped slots on scour around a bridge abutment. Water Practice & Technology, 16(3), pp: 935-945. https://doi.org/10.2166/wpt.2021.037.
30. Koohsari A, Hamidi M, (2021). Experimental study of the effect of mining materials downstream of bridge pier on scour profile with optimizing distance approach. Journal of Water and Soil Conservations, 28(3), pp: 1-26. 10.22069/JWSC.2022.19400.3490.
31. Ebrahimi T, Hamidi M, Rahmani Firoozjaiee A, Khavasi E, (2021). Numerical investigation of scour around a cylindrical pier in laboratory scale using Euler-Lagrange approach. Amirkabir Journal of Mechanical Engineering, 53(1 (Special Issue)), pp: 411-426. 10.22060/MEJ.2019.16679.6418.
32. Sadeqlu M, Hamidi M, (2022). Numerical investigation of the cylindrical bridge pier scour reduction by installing a group of two submerged vanes. Irrigation and Drainage Structures Engineering Research, 22(85), pp: 91-114. https://doi.org/10.22092/idser.2022.357739.1502.
33. Valela, C, Rennie CD, Nistor I, (2022). Improved bridge pier collar for reducing scour. International Journal of Sediment Research, 37(1), pp: 37-46. https://doi.org/10.1016/j.ijsrc.2021.04.004.
34. Khalili AM, Hamidi M, Dadamahalleh PA, (2023). Introducing Countermeasures for Reducing Bed Scour of Mountainous Rivers, 1st International Conference on Sustainable Mountain, 11&12 December 2023, University of Mohaghegh Ardabili.
35. Khalili AM, Hamidi M, Dadamahalleh PA, (2023). Reviewing Ice Covering Effect on Bridge Pier Scour Morphology at Cold Climate, 1st International Conference on Sustainable Mountain, 11&12 December 2023, University of Mohaghegh Ardabili.
36. Raudkivi AJ, Ettema R, (1983). Clear water scour at cylindrical piers. Journal of Hydraulic Engineering, 109(3), 338-350. https://doi.org/10.1061/(ASCE)0733-9429(1983)109:3(338).
37. Mahdian Khalili A, Hamidi M, (2023). Time evolution effect on the scour characteristics downstream of the sluice gate with the submerged hydraulic jump in a laboratory model. Journal of Hydraulic Structures 9(2), pp: 32-47. 10.22055/JHS.2023.43499.1249.
38. Hamidi M, Mohammadhoseyni F, (2020). Numerical Investigation of the Effect of Stilling Basin Length on Flow Energy Dissipation (Case Study of the Chaili Dam Spillway). Irrigation and Water Engineering, 11(1), pp: 66-86. 10.22125/IWE.2020.114954.
39. Biabani S, Hamidi M, Navayi Neya B, (2019). Numerical simulation of the chute convergence effects on forming the transverse wave in flood evacuation systems. Journal of Hydraulics, 14(3), pp: 67-84. 10.30482/JHYD.2019.174636.1373.